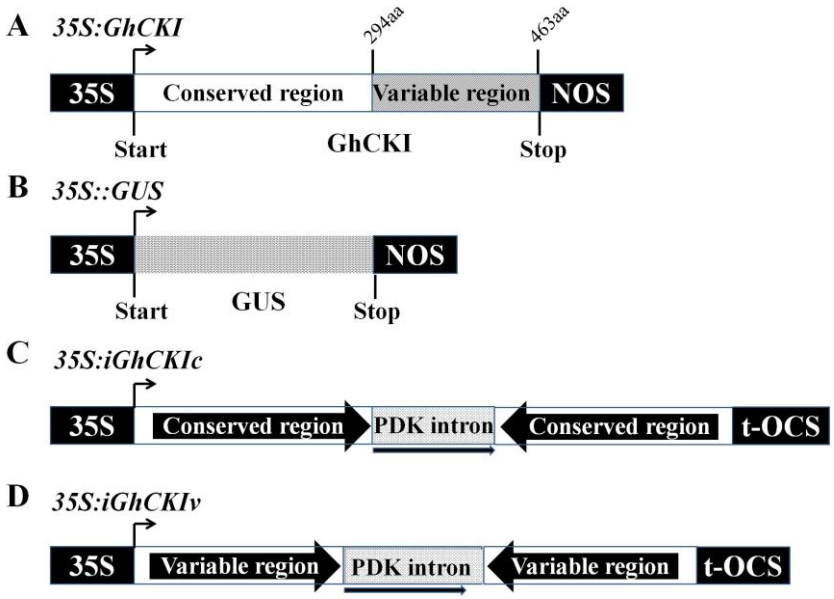

Figure S1: Constructs used for cotton and Arabidopsis transformation.

(A) and (B) Constructs for constitutive expression of *GhCKI* (*35S:GhCKI*) (A) and *GUS* (*35S::GUS*) (B). (C) and (D) Constructs for constitutive interference of *GhCKI* conserved (*35S:iGhCKIc*) and variable regions (*35S:iGhCKIv*), respectively. 35S, promoter of cauliflower mosaic virus; NOS, nopaline synthase; bent arrows, translation start.

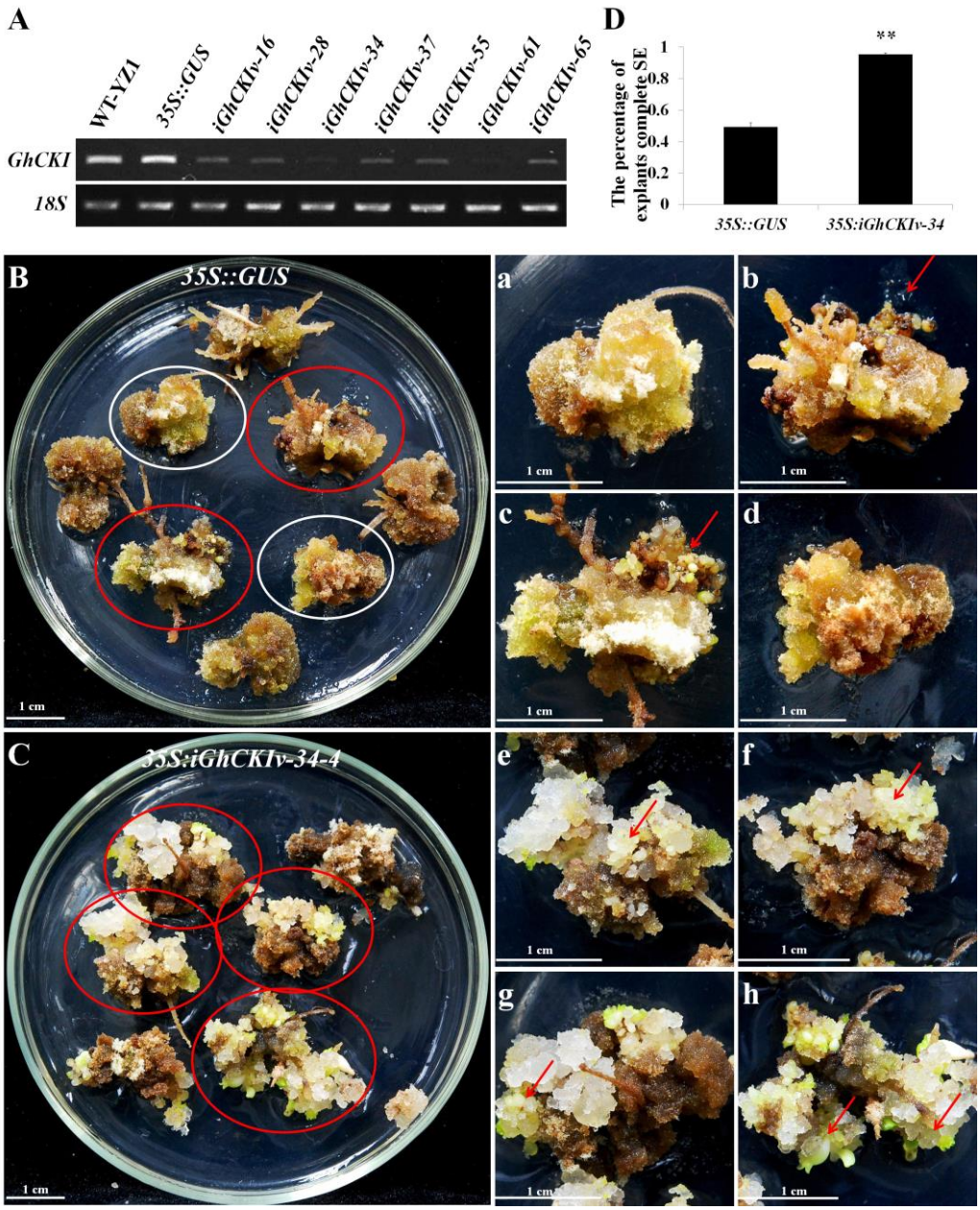

Figure S2: Comparison of embryogenic callus (EC) formation in the control and *GhCKI* variable region RNAi transformants. (A) RT-PCR analysis of *GhCKI* expression levels in hypocotyls among the seven transgenic lines: 28, 34, and 61 exhibited the lowest expression, line 16 exhibited moderate expression, 37, 55, 65 exhibited slightly decreased expression, compared with wild-type (WT-YZ1) and *35S::GUS* control plants. (B) and (C) Observation of callus phenotype variations in the control *35S::GUS* (B) and *GhCKI* variable region RNAi (*35S:iGhCKIv-34-4*) (C) transformants, respectively. (a) to (d) Highlight of A showing EC and somatic embryos formed from partial explants of the *35S::GUS* transgenic line. (e) to (h)

Highlight of B showing highly EC and somatic embryos formation from *35S:iGhCKIv-34-4* transgenic line. White and red cycles in B indicate (a and d) and (b and c), respectively; Red cycles in C indicate (e to h); Asterisks (b, c, e, f, g, h) indicate EC and somatic embryos; Bars, 1 cm.

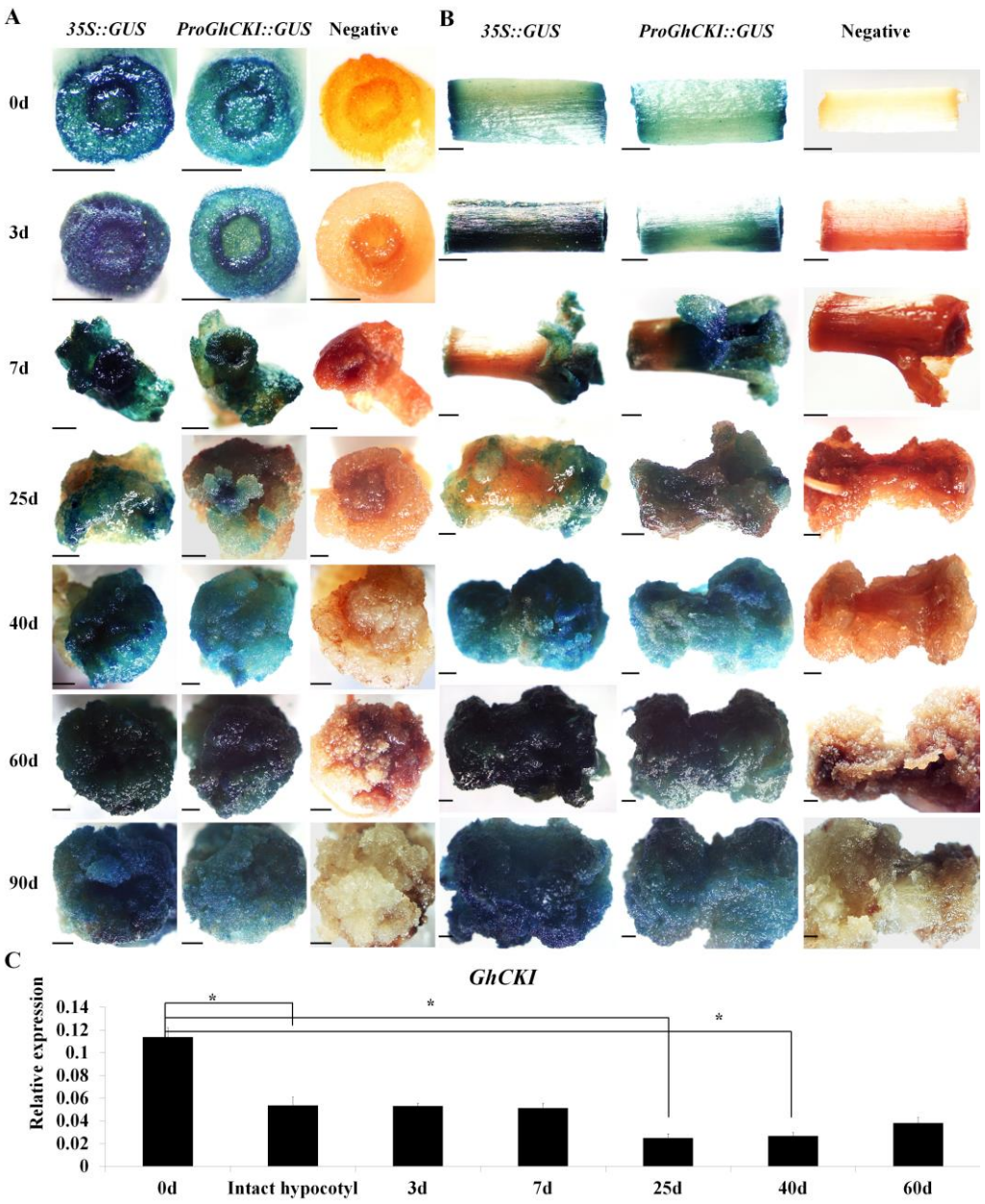

Figure S3: Expression pattern of *GhCKI* during SE.

(A) and (B) GUS staining analysis of T3 explants derived from *35S::GUS* and *ProGhCKI::GUS* transgenic lines at different culture stages. High accumulation of GUS protein during the entire SE process in *35S::GUS* transgenic explants was

detected. However, lower GUS activity was detected in *ProGhCKI::GUS*, especially in 25-d, 40-d, 60-d, and 90-d explants. Negative presented the null plants segregated from T1 line of *ProGhCKI::GUS* transgenics. 0 d-90 d, explants induced on the medium for 0 d to 90 d. Bars, 1 mm.

(C) Analysis of *GhCKI* expression by quantitative RT-PCR in wild type YZ1 explants at different induction stages. *GhCKI* expression decreased in 25 d to 60 d explants compared to WT 0 d (no cut) (hypocotyl of five-day-old seedlings of WT was not cut into sections). In addition, the *GhCKI* expression in WT 0 d (cut) (hypocotyl of five-day-old seedlings of WT was cut into sections) was significantly higher than that in WT 0 d (no cut), indicating *GhCKI* expression was induced by wounding. Asterisks (C) indicate statistically significant differences (** P<0.01, student's t test).

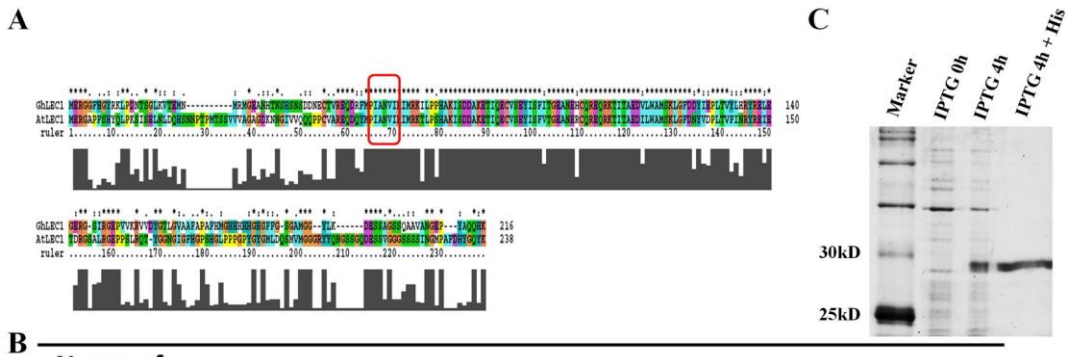

B

Name of probe	Sequence of probe
B1	GCTTCGATACGATCAAATCACCTGAGTGAGAACATAATTTTTTTTTGCTTTTTTA
B2	GAGATTGAAAATTAAGCTAATTTATTTGTTTTTTTTAGATAGTGATAGGAAAAAA
B3	ATAGAATTATGATTTCGTAGCTACTTTTCCTCCTTTTCTTTCTTCTTCGCATT
B4	TAGATTCTTCTTTTATTTTATTTTTTTTAGATTTTTTTTACTTGATTGATC
B5	AGCCTAACCTAACCCTAGGTTTTTTTTTGGTGTTCTTGTTAATTTTGTAT
B6	TTGTTTGTGGTTTAAGGTAAAAGACGGAATTCTAGGTTTTTTCTCC

Figure S4: Isolation and expression of GhLEC1. (A) Alignment analysis of GhLEC1 and AtLEC1 amino acid sequences. The GhLEC1 protein is similar to the AtLEC1 protein at the 53% amino acid level. The DNA binding region PIANV is boxed, which is known to serve as a conserved DNA binding domain for HAP3s. (B) Six distinct regions of B region of *ProGhCKI* sequence. (C) Detection and purification of GhLEC1 protein. IPTG 0h or 4h are *Escherichia coli* BL21 strain containing pET-28a-*GhLEC1* which was induced by IPTG

(isopropyl-1-thio-b-D-galactopyranoside) for 0 h or 4 h. IPTG 4h + His indicates the induced GhLEC1-His protein was purified.

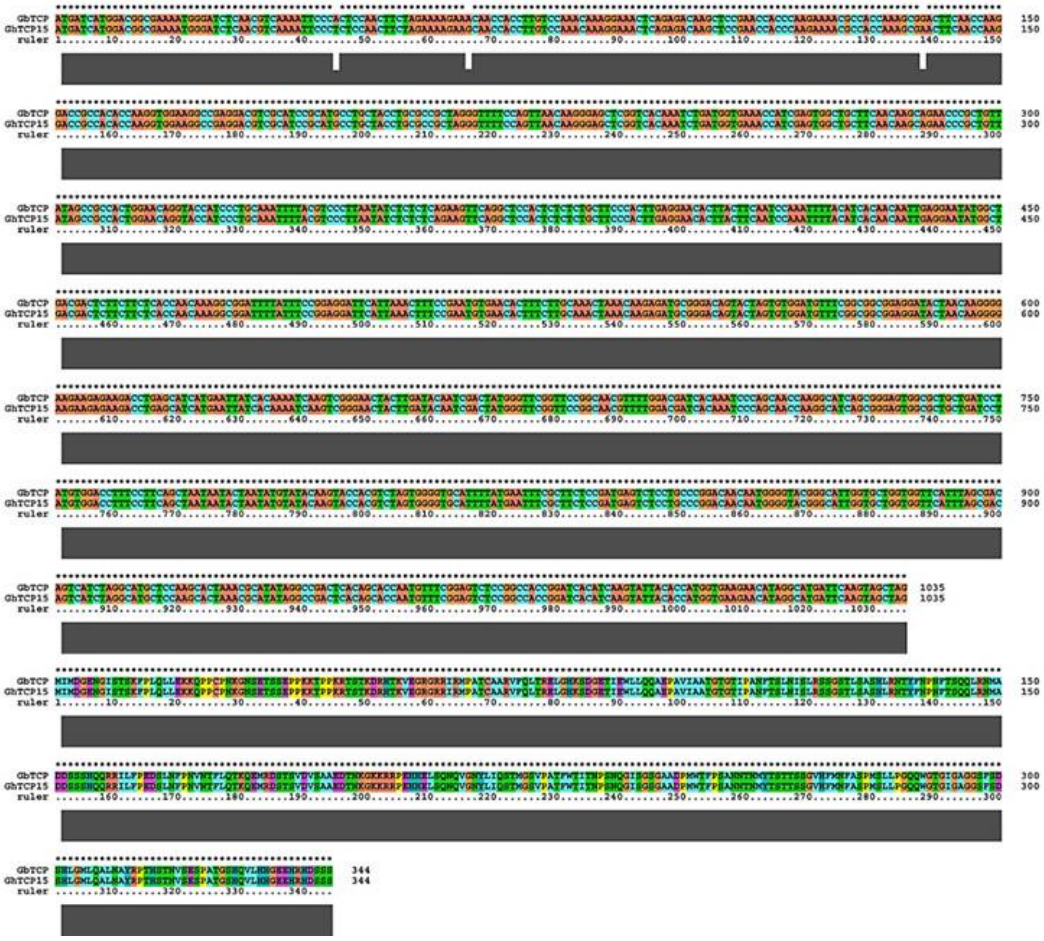

Figure S5: Sequence alignment between GbTCP and GhTCP15. Three base pairs were different between *GbTCP* and *GhTCP15* cDNA sequences, and GbTCP is 100% homologous to GhTCP15 at amino acid level.

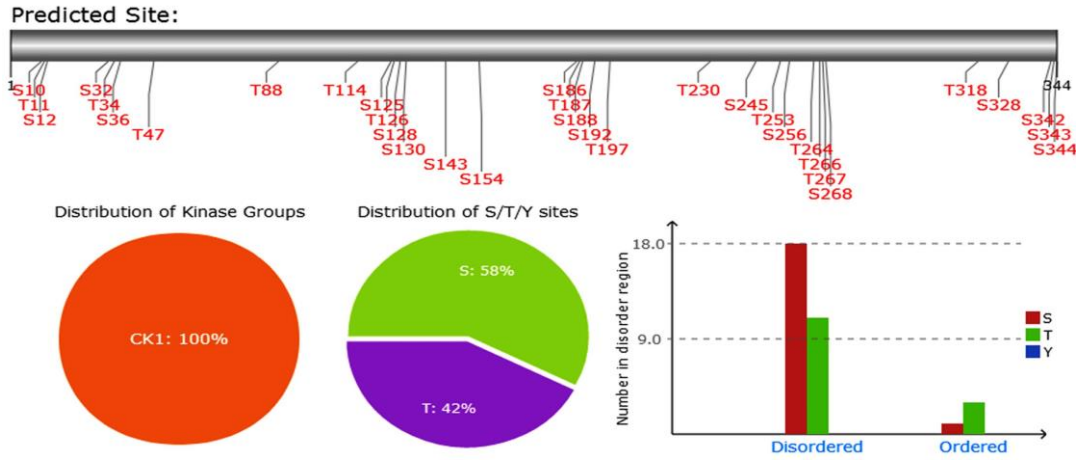

Figure S6: Predicted phosphorylation sites by CKI in GhTCP15. The CKI phosphorylation sites in GhTCP15 were determined by group-based prediction system 3.0.

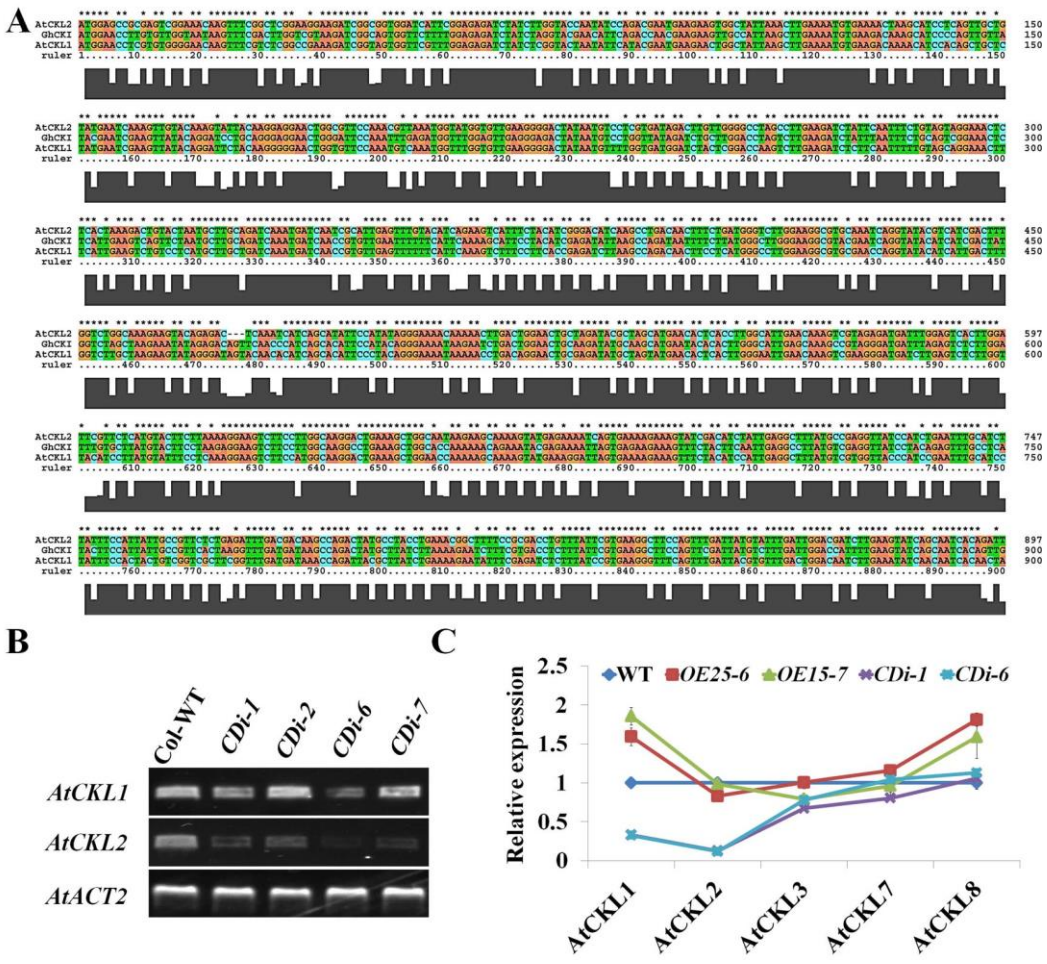

Figure S7: Downregulation expression of *GhCKI* homologus genes in Arabidopsis by RNAi. (A) Sequence alignment among *GhCKI*, *AtCKL1*, and *AtCKL2*. The

conserved domain of *AtCKL1* and *AtCKL2* showed a high degree of nucleotide sequence conservation with *GhCKI.* (B) RT-PCR analysis of *AtCKL1* and *AtCKL2* in young seedling in four transgenic lines. The expression of *AtCKL1* was decreased in *CDi-1* and *CDi-6*, no significant differences in *CDi-2* and *CDi-7*. Expression of *AtCKL2* was strongly reduced in four lines, and *CDi-1* and *CDi-6* exhibited the lowest expression. (C) Relative expression levels of *AtCKLs* in WT, *OE25-6, OE15-7, CDi-1* and *CDi-6*.

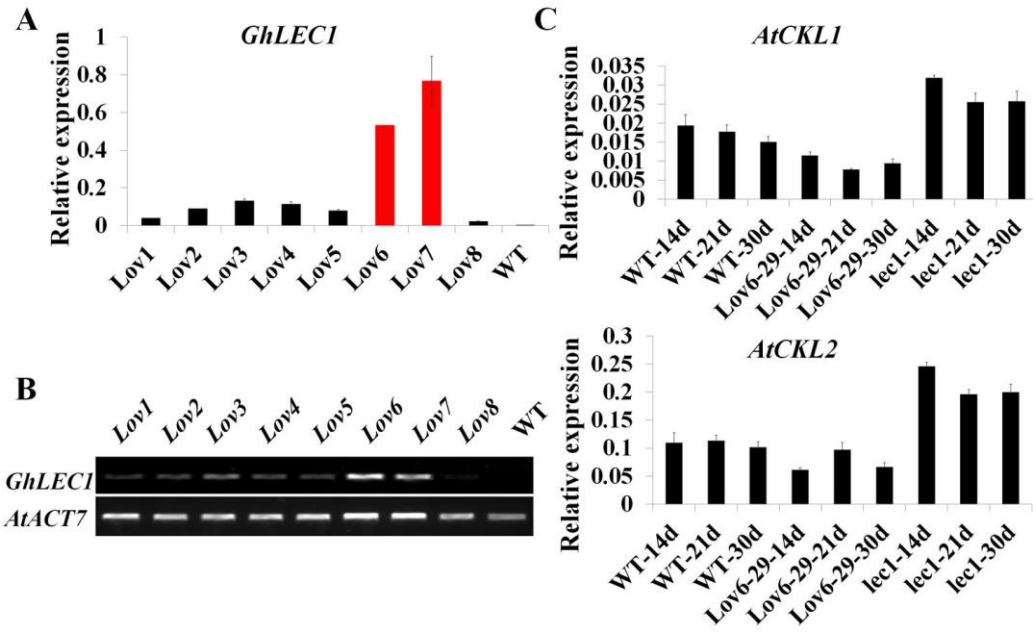

Figure S8: Isolation of ectopically overexpressed *GhLEC1* Arabidopsis plants. (A) and (B) Analysis of the expression of *GhLEC1* in wild-type and *GhLEC1* overexpressing lines (*Lov1* to *8*) by qRT-PCR (A) and RT (B). *Lov6* and *Lov7* were isolated as the highest expression lines, *AtACT7* was used as a control. (C) qRT-PCR analysis of *AtCKL1* and *AtCKL2* levels in callus of wild-type, overexpressing lines (*Lov6-29*), and *lec1-1* mutants at induction for 14 d, 21 d, and 30 d. The expression of *AtCKL1* and *AtCKL2* was down-regulated by overexpressing *GhLEC1* and up-regulated in *lec1-1* mutants.

Line / Time	WT FW(g/5callus)	*OE25-6* FW(g/5callus)	*OE15-7* FW(g/5callus)	*CDi-1* FW(g/5callus)	*Lov6-29* FW(g/5callus)	*lec1-1* FW(g/5callus)	*OETCP6-9* FW(g/5callus)	*tcp14/15* FW(g/5callus)
0d	9.71E-05 ±5.25E-06	9.97E-05 ±2.1E-06	1.48E-04 ±2.73E-06	9.08E-05 ±1.44E-06	9.41E-05 ±1.26E-06	7.54E-05 ±1.24E-06	1.01E-04 ±8.58E-07	1.04E-04 ±1.6E-06
SSR (*P*<0.05)	bcd	bcd	e	b	bc	a	cd	d
21d	3.8E-02 ±7.22E-04	3.95E-02 ±1.05E-03	7.79E-02 ±2.23E-03	3.09E-02 ±8.37E-04	3.43E-02 ±5.61E-04	6.01E-02 ±6.01E-04	6.92E-02 ±1.65E-03	3.58E-02 ±1.31E-03
SSR (*P*<0.05)	b	b	e	a	ab	c	d	ab
30d	5.19E-02 ±1.01E-03	5.34E-02 ±1.04E-03	1.1E-01 ±3.54E-03	3.6E-02 ±8.15E-04	3.94E-02 ±4.45E-04	7.08E-02 ±1.34E-03	9.79E-02 ±1.95E-03	4.3E-02 ±9.1E-04
SSR (*P*<0.05)	B	B	E	A	A	C	D	A
(21d-0d) /0d	381.29 ±6.97	390.83 ±13.33	530.32 ±13.35	336.18 ±10.04	363.72 ±8.66	785.53 ±19.22	687.21 ±14.62	351.28 ±17.62
SSR (*P*<0.05)	B	B	C	A	A	E	D	A
(30d-21d) /21d	0.379 ±0.053	0.384 ±0.045	0.406 ±0.094	0.152 ±0.021	0.153 ±0.034	0.181 ±0.042	0.405 ±0.045	0.199 ±0.069
SSR (*P*<0.05)	BC	BC	C	A	A	AB	BC	AB

Line / Time	WT DW(g/5callus)	*OE25-6* DW(g/5callus)	*OE15-7* DW(g/5callus)	*CDi-1* DW(g/5callus)	*Lov6-29* DW(g/5callus)	*lec1-1* DW(g/5callus)	*OETCP6-9* DW(g/5callus)	*tcp14/15* DW(g/5callus)
0d	9.71E-05 ±5.25E-06	9.97E-05 ±2.1E-06	1.48E-04 ±2.73E-06	9.08E-05 ±1.44E-06	9.41E-05 ±1.26E-06	7.54E-05 ±1.24E-06	1.01E-04 ±8.58E-07	1.04E-04 ±1.6E-06
SSR (*P*<0.05)	BCD	BCD	E	B	BC	A	CD	D
21d	2.67E-03 ±1.63E-04	2.69E-03 ±1.59E-04	5.28E-03 ±1.86E-04	2.15E-03 ±1.22E-04	2.5E-03 ±1.23E-04	3.55E-03 ±1.5E-04	4.29E-03 ±3.73E-04	2.47E-03 ±1.28E-04
SSR (*P*<0.05)	A	AB	D	A	A	C	C	A
30d	3.63E-03 ±1.26E-04	3.71E-03 ±8.39E-04	7.43E-03 ±2.89E-04	2.56E-03 ±1.18E-04	2.84E-03 ±1.12E-04	4.61E-03 ±1.7E-04	6.17E-03 ±3.94E-04	3.2E-03 ±2.04E-04
SSR (*P*<0.05)	BC	BC	E	A	AB	C	D	AB
(21d-0d) /0d	25.82 ±1.69	25.76 ±1.78	35.18 ±2.09	22.41 ±1.3	27.54 ±1.45	45.52 ±2.48	41.64 ±3.58	23.32 ±1.61
SSR (*P*<0.05)	AB	AB	BC	A	AB	C	C	AB
(30d-21d) /21d	0.388 ±0.045	0.378 ±0.072	0.428 ±0.071	0.176 ±0.021	0.164 ±0.039	0.295 ±0.048	0.401 ±0.031	0.273 ±0.052
SSR (*P*<0.05)	BC	BC	C	A	A	B	C	B

Figure S9: Effects of *GhLEC1*, *GhCKI*, and *GhTCP15* on callus mass during SE.

The fresh and dry weight and the proliferation rates of callus were determined for WT-Col, *OE25-6*, *OE15-7*, *CDi-1*, *Lov6-29*, *lec1-1*, *OETCP6-9*, and *tcp14/15* after cultured for 21 d and 30 d on the same plate. The data represent the means ± s.e.m of 3 biologically independent experiments. Values not sharing a common letter were considered statistically significant (shortest significant ranges, SSR; $p<0.05$).

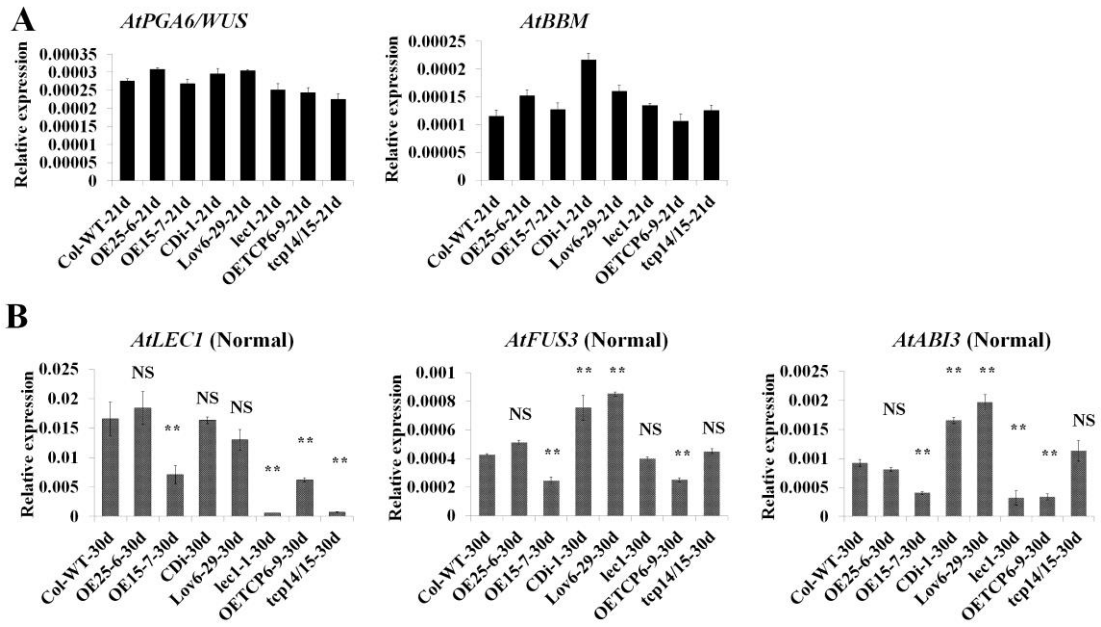

Figure S10: GhLEC1-GhCKI-GhTCP15 governs the switch from cell proliferation to cell differentiation by regulating the homeostasis of auxin.

(A) and (B) Expression levels for embryonic cell identity (A) and somatic embryo formation (B) related genes were validated by qRT-PCR in Col-WT, *OE25-6*, *OE15-7*, *lec1-1*, *OETCP6-9* and *tcp14/tcp15* Arabidopsis callus cultured for 21 d (A) and 30 d (B). *PGA6/WUS*, *Plant Growth Activator* 6/*WUSCHEL*; *BBM*, *BABY BOOM*; *LEC1*, *LEAFY COTYLEDON1*; *FUS3*, *FUSCA3*; *ABI3*, *ABA INSENSITIVE3*. Data in (B) represent the means ± s.e.m of biologically independent experiments ($n \geq 3$). Asterisks indicate statistically significant differences between different lines and wild-type (**; $P<0.01$, NS; not significant, t-test).

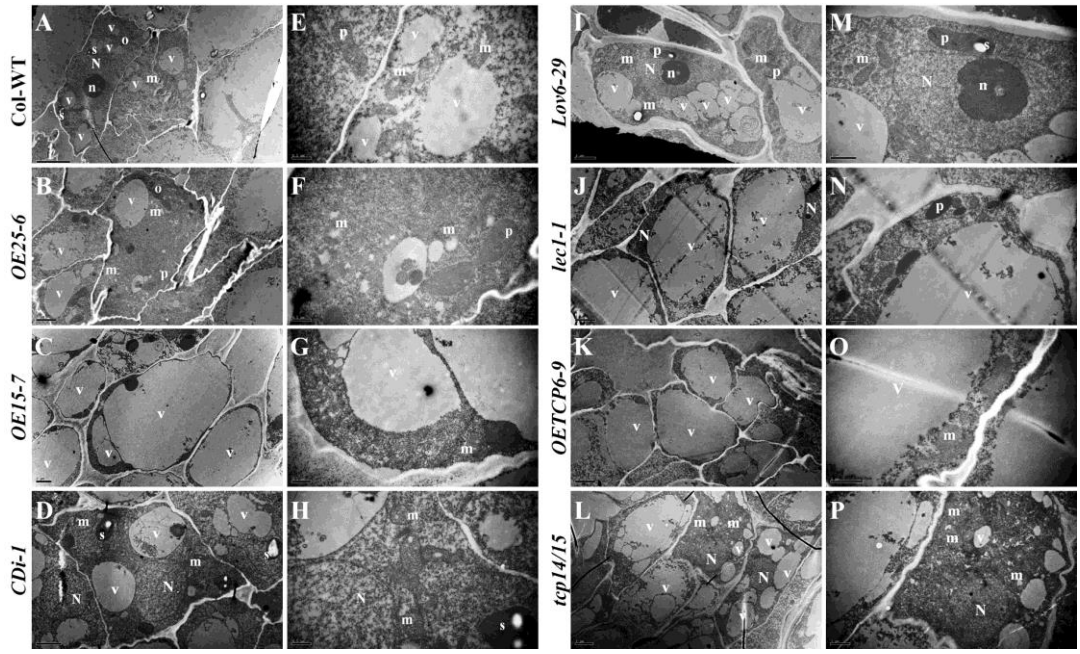

Figure S11: TEM analyses of cultures after induction for 30 d in WT-Col, *OE25-6, OE15-7, CDi-1, Lov6-29, lec1-1, OETCP6-9,* and *tcp14/15.* (A) to (D) Cross sections of Col-WT (A), *OE25-6* (B), *OE15-7* (C), and *CDi-1* (D). (E) to (H) Magnified view of the cytoplasmic region in (A) to (D), respectively. (I) to (L) Cross-sections of *Lov6-29* (I), *lec1-1* (J), *OETCP6-9* (K), and *tcp14/15* (L). (M) to (P) Magnified view of the cytoplasmic region in (A) to (D), respectively. m, mitochondria; v, vacuole; s, starch granule; o, orbicule; P, plasmid; n, nucleolus; N, nucleus. Bars, 5 μm in (A), 2 μm in (B to D) and (I to L), 0.5 μm in (E to H), and 1 μm in (M to P).